Bull. Mater. Sci., Vol. 35, No. 2, April 2012, pp. 183–189. © Indian Academy of Sciences.

Influence of pH and bath composition on properties of Ni–Fe alloy films synthesized by electrodeposition

XINGHUA SU[1] and CHENGWEN QIANG[2,*]

[1]School of Materials Science and Engineering, Chang'an University, Xi'an 710061, China
[2]China and Institute of Modern Physics, Chinese Academy of Science, Lanzhou 730000, China

MS received 1 April 2011; revised 14 May 2011

Abstract. **Fe–Ni films were electrodeposited on ITO glass substrates from the electrolytes with different molar ratio of Ni^{2+}/Fe^{2+} and different pH values (2·1, 2·9, 3·7 and 4·3) at 25°C. The properties of Fe–Ni alloy films depend on both Ni^{2+} and Fe^{2+} concentrations in electrolyte and pH values. The content of Ni increases from 38% to 84% as the mole ratio of $NiSO_4/FeSO_4$ increasing from 0·50/0·50 to 0·90/0·10 in electrolyte and slightly decreases from 65% to 42% as the pH values increase from 2·1 to 4·3. The X-ray diffraction analysis reveals that the structures of the films strongly depend on the Ni content in the binary films. The magnetic performance of the films shows that the saturation magnetization (M_s) decreases from 1775·01 emu/cm^3 to 1501·46 emu/cm^3 with the pH value increasing from 2·1 to 4·3 and the saturation magnetization (M_s) and coercivity (H_c) move up from 1150·44 emu/cm^3 and 58·86 Oe to 2498·88 emu/cm^3 and 93·12 Oe with the increase of Ni^{2+} concentration in the electrolyte, respectively.**

Keywords. **Fe–Ni film; electrodeposition; anomalous codeposition; magnetic property.**

1. Introduction

Magnetic films have attracted much attention due to their potential applications in small electric components, such as radio-frequency thin film inductors and computer read/write heads. Single ferromagnetic films of transition metals such as nickel, cobalt, iron and their alloys are typical magnetic materials applicable in soft-magnetic and anisotropic magnetoresistance (AMR) (Korenivski 2000; Siritaratiwat *et al* 2000; Valeri *et al* 2001; Jartych *et al* 2002; Chisholm *et al* 2007). These materials are important for applications as well as for fabrication. For example, films of Ni–Fe binary alloy are used for recording, memory and storage devices (Romankiw *et al* 1970; Venkatasetty 1970).

The most common film growth processes such as sputtering, molecular beam epitaxy require high or ultrahigh vacuum. It is also possible to prepare such ferromagnetic films by electroplating, which does not need any vacuum system. Moreover, it has more advantages like low cost and easy control by changing the electrodeposition parameters in the experiment. Quantities of metallic coatings were prepared by the electroplating method, such as Ni–Co (Marikkannu *et al* 2007), Cu–Sn (Lodhi *et al* 2007), Zn–Co (Chen and Sun 2001) and Zn–Ni (Beltowska-Lehman *et al* 2002), composite films of Ni–SiC (Gyftou *et al* 2008) and Fe–Cr–P (Li *et al* 2008) were also prepared by the electro-plating method. In electrodeposition the growth mechanism, morphology and micro-structural properties of the film depend on electrodeposition conditions such as electrolyte composition, electrolyte pH and deposition potential. Electrodeposition of Fe–Ni alloy was classified as anomalous codeposition, because the less noble metal was deposited preferentially (Zech *et al* 1999). According to the earlier studies, the anomalous behaviour was caused by the preferential absorption of iron hydroxide on the cathode, which leads to higher deposition ratio of Fe than Ni (Krause *et al* 1997). However, this hypothesis could not explain experimental works. While, according to the new model, $NiOH^+$ and $FeOH^+$ formed from the hydrolysis of Ni^{2+} and Fe^{2+}, are discharged at the cathode surface. The anomalous codeposition is attributed to the high concentrations of $FeOH^+$ near electrode (Sasaki and Talbot 2000). The most comprehensive model of the Fe–Ni alloy electrodeposition was presented by Matlosz (1993), who proposed that reduction of each metal ion occurred through a two-step mechanism. The first step involved the adsorption of a monovalent intermediate and the next step was its reduction to the elemental state. Anomalous codeposition was carried out from the preferential surface coverage of the absorbed iron intermediate (Yin 1997; Sasaki and Talbot 2000). The difficulties introduced by anomalous codeposition inherent to the Fe–Ni alloy, has necessitated empirically developed coating bath, which typically contain different organic additives (Lieder and Biallozor 1985; Yin and Lin 1996; Harris *et al* 1999).

It is well known that the properties of Fe–Ni films are seriously affected by their compositions and structures (Osaka 1999), thus a reliable control of the composition and structure is an important issue in designing the magnetic functionality of these materials. Since the magnetic properties of

*Author for correspondence (qiangchw08@lzu.edu.cn)

Fe–Ni alloys are seriously affected by their compositions and structures (Passal 1966, 1967; Friemel 1966, 1967; Beltowska-Lenman and Riesenkampf 1980; Schwarzacher and Lashmore 1996; Osaka *et al* 1998; Osaka 1999), a reliable control of the composition and textural properties (e.g. crystalline structures, morphologies, roughness, etc) through plating is an important issue in designing the magnetic functionality of these materials. For example, the nanostructured permalloy (i.e. $Ni_{81}Fe_{19}$ alloy) has been found to be a high-quality magnetic recording material (Chueng *et al* 1994a, b). Zhang and Ivey (2004) studied magnetic properties of Ni–Fe–Co alloys and demonstrated that the magnetic properties were sensitive to the composition and pH levels. Additionally, they have previously reported that Fe–Co films with different morphology and Co content were successfully electrodeposited on ITO glasses from the electrolyte containing different Co^{2+} and pH values. The result shows that the saturation magnetization of the Fe–Co alloy films reaches a maximum value of 2974·03 emu/cm^3 and coercivity (H_c) reaches a minimum value of 42·72 Oe of the Co: Fe=4:1. M_S reaches a maximum value of 2974·03 emu/cm^3 and H_C reaches a minimum value of 42·72 Oe of the Co: Fe=4:1 at pH=2·9 (Qiang *et al* 2010). In this study, the structure and magnetic property of electrodeposited Fe–Ni films were investigated as a function of the molar ratio of Ni^{2+}/Fe^{2+} and pH values in electrolyte. It was clearly observed that the surface morphology and magnetic property were changed significantly with the electrolyte pH and different molar ratios of Ni^{2+}/Fe^{2+} in electrolyte.

2. Experimental

In this study, Ni–Fe films were grown from an electrolyte containing Ni^{2+} and Fe^{2+} ions under potentiostatic conditions. Electrodeposition was performed in an electrochemical cell with three electrodes using a potentiostat. ITO glass with an area of 3 cm^2 was used as substrates. Before deposition, ITO glass was first cleaned with acetone for 30 min and then alcohol for 30 min, finally rinsed in distilled water. The reference electrode was a saturated calomel electrode (SCE). The anode was iron plate of dimension, 3 cm^2. Prior to deposition, the iron plate was first mechanically polished and then washed in dilute sulfuric acid and distilled water. Both electrodes were immersed in the same electrolyte.

The compositions of the electrolytes with different molar ratios of Ni^{2+}/Fe^{2+} were shown in table 1, together with major plating parameters. The total concentration of ferrous sulfate [$FeSO_4{\cdot}7H_2O$] and nickel sulfate [$NiSO_4{\cdot}6H_2O$] was kept at 0·20 M. All chemicals were of reagent grade and dissolved in distilled water. Electrolytes of the same composition but with different pH values were also prepared for comparison. The electrolyte composed of 0·12 M nickel sulfate [$NiSO_4{\cdot}6H_2O$], 0·08 M ferrous sulfate [$FeSO_4{\cdot}7H_2O$], 0·4 M boric acid [H_3BO_3], 1·7 mM ascorbic acid [$C_6H_8O_6$] and 1·38 mM thiourea [CH_4N_2S] with different pH values of 2·1, 2·9, 3·7 and 4·5 adjusted by sodium hydroxide [NaOH] and sulphuric acid [H_2SO_4]. Ni–Fe films were deposited at a cathode potential of −1·5 V vs SCE. All the films were plated at a current density of 0·5 A·dm^{-2} at 25°C without stirring.

Table 1. Constitution and operating conditions of plating bath.

Reagents	Concentration
$FeSO_4{\cdot}7H_2O$	0·10,0·08,0·06,0·04,0·02 M dm^{-3}
$NiSO_4{\cdot}6H_2O$	0·10,0·12,0·14,0·16,0·18 M dm^{-3}
H_3BO_3	0·40 M dm^{-3}
Ascorbic acid	1·70 mM dm^{-3}
Thiourea	1·38 mM dm^{-3}
Temperature	Room temperature
pH values	2·9
Current density	0·5A dm^{-2}
Plating duration	480 s
Anode	Iron plate
Cathode	ITO glass

The chemical composition of the films was analysed by inductively coupled plasma atomic emission spectrometry (ICP-AES). X-ray diffraction (XRD) measurements were performed on Rigaku D/Max-2400 X-ray diffractometer using Cu Kα radiation (40 kV, 60 mA). XRD data were recorded in a range from 25° to 90° with a step width of 0·02° and a counting time of 3 s per step. The morphology of the films was analysed on a Hitachi S-4800 field emission scanning electron microscope (SEM) operating at an acceleration voltage of 5 kV. The magnetic properties of the $Fe_{1-x}Ni_x$ films were measured by a Lake Shore 7304 vibrating sample magnetometer at room temperature.

3. Results and discussion

3.1 *Effect of Ni % in electrolyte*

3.1a *ICP analysis*: ICP–AES measurement of the obtained films shows significant differences that exist between the actual compositions and the ratio of precursor electrolyte. The total concentration of ferrous sulfate [$FeSO_4{\cdot}7H_2O$] and nickel sulfate [$NiSO_4{\cdot}6H_2O$] was kept at 0·20 M. By changing the molar ratio of Ni^{2+}/Fe^{2+} in the reaction electrolyte from 0·50/0·50 to 0·90/0·10, the Ni content x in the films ranges from 38% to 84%. Meanwhile, the Fe content in the films decreases from 62% to 16%. As can be seen in figure 1, the Ni content is always lower than that in electrolytes demonstrating the existence of anomalous codeposition during the electrodeposition process. According to Matlosz's (1993) definition, the codeposition of iron-group metals (e.g. Fe, Co and Ni) is widely recognized as an anomalous electroplating type. The sequence of metal hydroxide ions with respect to increase in the adsorption ability is $Ni(OH)^+ < Fe(OH)^+$ (Yin and Lin 1996). The reaction mechanism is generally processed as following (Yin and Lin 1996; Harris *et al* 1999):

$$2H_2O + 2e^- \leftrightarrow H_2 + 2OH^-, \quad (1)$$

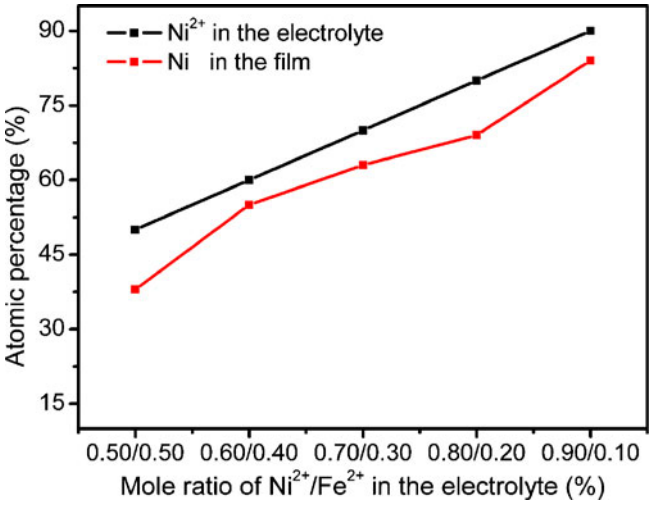

Figure 1. Effect of molar ratio of $NiSO_4/FeSO_4$ in electrolyte on film composition.

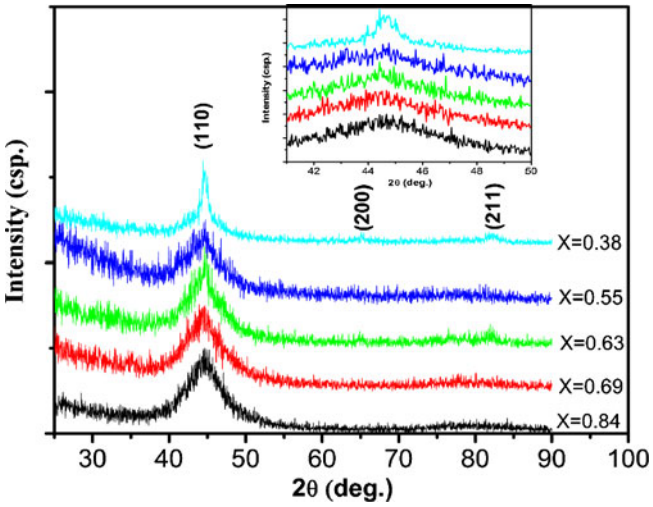

Figure 2. XRD patterns of $Fe_{1-x}Ni_x$ films with Ni contents of $x = 0{\cdot}38, 0{\cdot}55, 0{\cdot}63, 0{\cdot}69$ and $0{\cdot}84$. The inset shows the magnified (110) diffraction peaks of XRD patterns.

$$M^{2+} + OH^- \leftrightarrow MOH^+, \quad (2)$$

$$MOH^+ \rightarrow (MOH)^+_{ads}, \quad (3)$$

$$(MOH)^+_{ads} + 2e^- \leftrightarrow M + OH^-, \quad (4)$$

where M indicates iron and nickel atoms. Although many attempts have been made to explain the anomalous codeposition of alloys, there is still no universally accepted theory.

3.1b *XRD analysis*: The XRD patterns of the prepared $Fe_{1-x}Ni_x$ films with different Ni contents, x, are shown in figure 2. The three diffraction peaks located at about 45·6°, 64·9° and 82·3° are corresponding to FeNi (110), FeNi (200) and FeNi (211) of cubic structure. As shown in figure 2, the diffraction peaks of FeNi (110) shows stronger preferred orientation than that of FeNi (211) and FeNi (200) at any Ni content x. From the inset in figure 2, we can see that the diffraction peaks in the XRD patterns shift slightly towards low angles with increasing Ni content x, indicating increased lattice constant with increasing Ni content x. This can be attributed to the large atom radius of Ni (0·162 nm) as compared to the atom radium of Fe (0·110 nm). The incorporation of large atoms into the lattice of the film would expand the lattice and increase the lattice parameters (Kakatkar *et al* 1996; Tilak *et al* 1997). The average grain size for all the Fe–Ni films estimated from the diffraction peak widths by Scherrer equation increases from 104 to 294 nm with the Co content x increasing from 0·38 to 0·84. On the basis of above discussion, the structure of the deposited Fe–Ni films strongly depends on both Ni^{2+} and Fe^{2+} concentrations in the electrolyte.

3.1c *SEM analysis*: Figure 3 displays the surface morphologies of $Fe_{1-x}Ni_x$ films with different Ni contents ($x =$ 0·38, 0·55, 0·63, 0·69 and 0·84). Although the morphological investigation indicated that all the films have similar grainy structure, it is clearly found that the morphologies of the films are significantly influenced by both Ni^{2+} and Fe^{2+} concentrations in the plating bath. With increased Ni, the surface of the films becomes more rough and have larger grains. The effect is attributed to different compositions. From the morphologies, we can see that size of the films increase from 100 nm to 300 nm with Ni content x increasing from 0·38 to 0·84. The average grain size determined by the SEM observations is in agreement with the average grain size estimated by XRD analysis, indicating that the granules in the Fe–Ni films observed by SEM are grains and crystallites.

3.1d *Magnetic property analysis*: Figure 4 shows the dependence of saturation magnetization (M_s) and coercivity (H_c) of the films deposited from the electrolyte containing different mole ratios of Ni^{2+} and Fe^{2+}. It can be seen that the saturation magnetization (M_s) moves up from 1150·44 emu/cm^3 to 2498·88 emu/cm^3 with the increase of Ni^{2+} concentration in the electrolyte. The increase of the saturation magnetization (M_s) can be attributed to the increase of Ni content in the deposited films which is consistent with the previous ICP analysis. The coercivity (H_c) decreases with Ni content x increasing from 0·38 to 0·55, reaches a minimum value of 43·14 Oe at $x = 0{\cdot}55$, and then increases with further increasing of x. The coercivity (H_c) may be effected by two factors. First, the existence of defects in the films. Second, the increase of Ni content in the films. In this group of experiment, the effect of defect can be neglected compared with the sharp increase of Ni in the films resulting in an increase of coercivity (H_c).

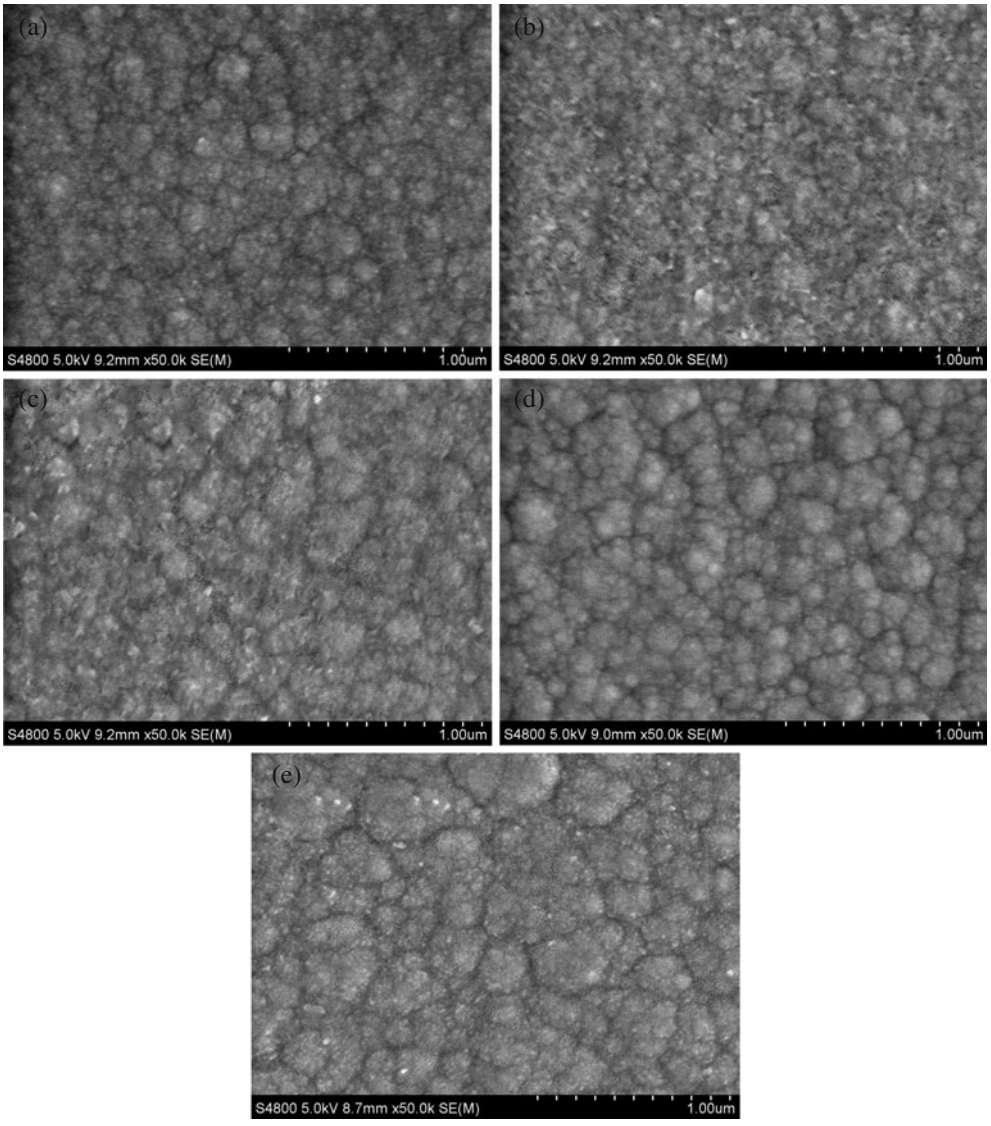

Figure 3. SEM images of Fe–Ni films deposited at different Ni contents (**a**) $Fe_{0.62}Ni_{0.38}$, (**b**) $Fe_{0.45}Ni_{0.55}$, (**c**) $Fe_{0.37}Ni_{0.63}$, (**d**) $Fe_{0.31}Ni_{0.69}$ and (**e**) $Fe_{0.16}Ni_{0.84}$.

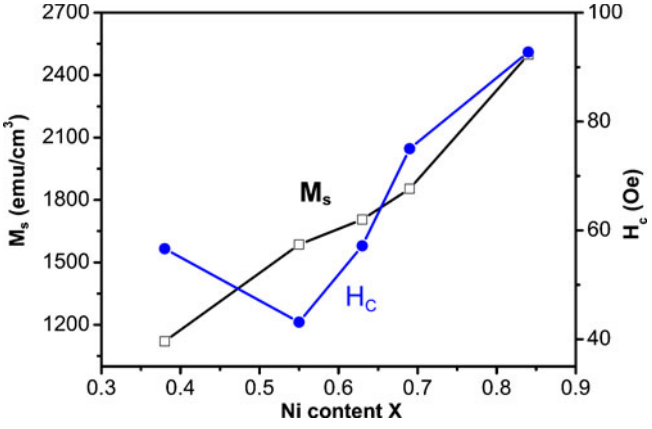

Figure 4. Dependence of saturation magnetization (M_S) and coercivity (H_C) of Fe–Ni films on Ni content x.

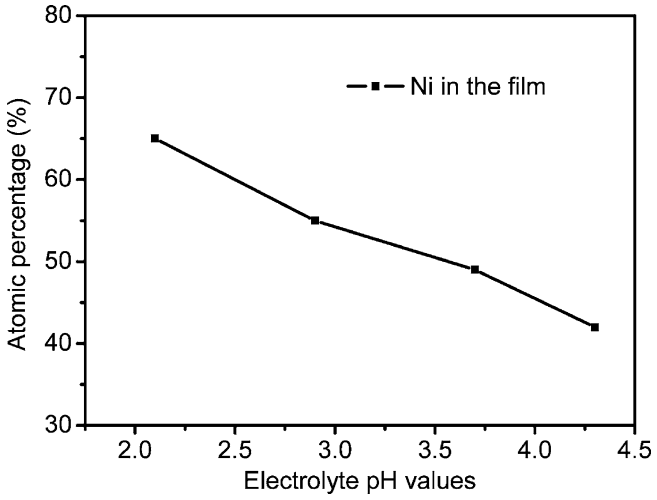

Figure 5. Dependence of Ni content in films on pH value.

3.2 *Effects of pH values*

3.2a *ICP analysis*: The effect of pH values on the composition of deposited films is shown in figure 5. It is found that the content of Ni in the deposited films falls from 65 to 42%, the content of Fe increases from 35 to 58% as the pH values vary from 2·1 to 4·3. The electrodeposition process is mainly dominated by anomalous codeposition. The electrodeposition process is mainly dominated by three factors: (i) the dissolution of the freshly deposited metal atoms on the substrate because of the acid condition in the electrolyte, (ii) the formation and absorption of metals hydroxides on the electrode surface and (iii) the anomalous electrodeposition of the metals. A lower pH value favours the dissolution of freshly deposited metals and depresses the formation and absorption of metal hydroxides, the process is predominated by the second factor except the anomalous electrodeposition resulting in a higher nickel content in the films due to the higher Ni^{2+} in the electrolyte. Nevertheless, a higher pH value favours the formation and absorption of metals hydroxides and depresses the dissolution of the freshly deposited metals; the process is predominated by the anomalous deposition of the metals resulting in a lower nickel content because of the preferential absorption of iron hydroxides in the electrolyte (Yin and Lin 1996; Harris *et al* 1999).

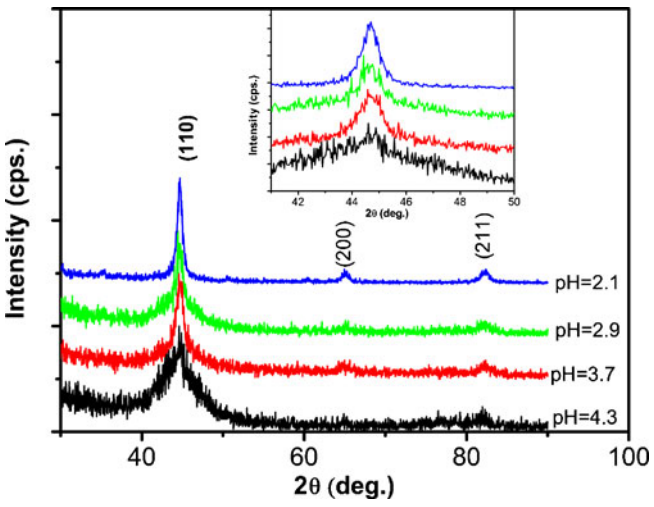

Figure 6. XRD patterns of Fe–Ni films deposited at different pH values.

3.2b *XRD analysis*: Figure 6 shows the XRD patterns of Fe–Ni films deposited at different pH values, the electrolyte containing 0·12 M $NiSO_4{\cdot}6H_2O$ + 0·08 M $FeSO_4{\cdot}7H_2O$ + 0·4 M H_3BO_3 + 1·7 mM $C_6H_8O_6$ + 1·38 mM CH_4N_2S at room temperature. The diffraction peaks corresponding to Fe–Ni alloys are found on all the curves, indicating the micro-crystalline structure of the films plated from the electrolytes of four pH values. As noticed in figure 6, no other diffraction peaks are found except the FeNi peaks located at about 45·6°, 64·9° and 82·3° corresponding to FeNi (110),

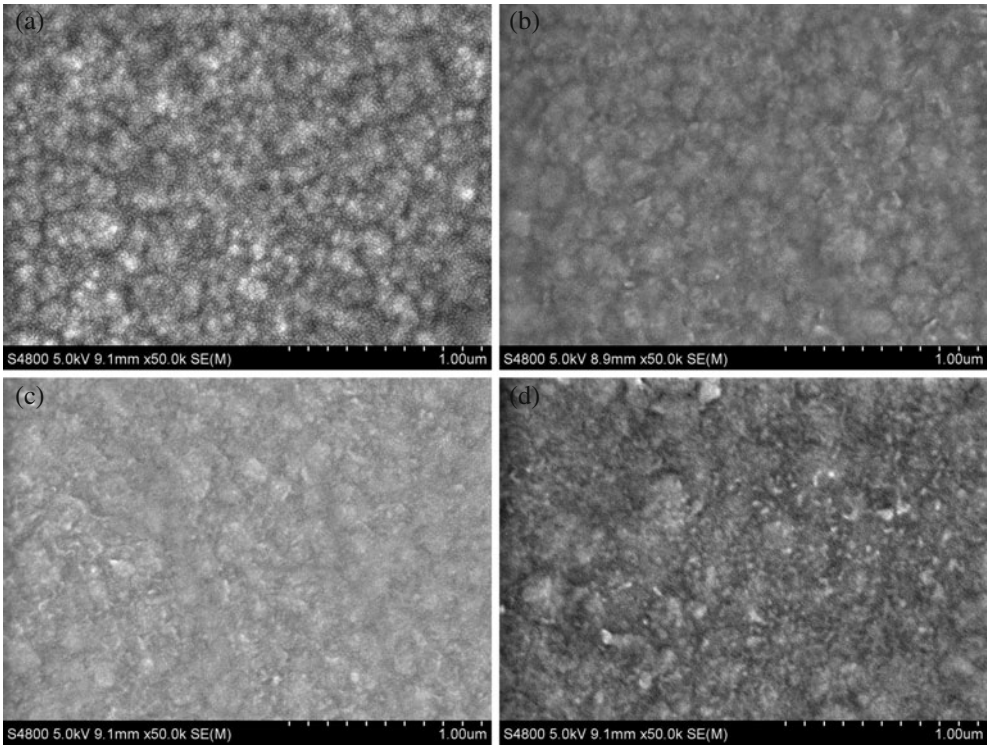

Figure 7. SEM images of Fe–Ni films deposited at different pH values (**a**) pH = 2·10, (**b**) pH = 2·90, (**c**) pH = 3·70 and (**d**) pH = 4·50.

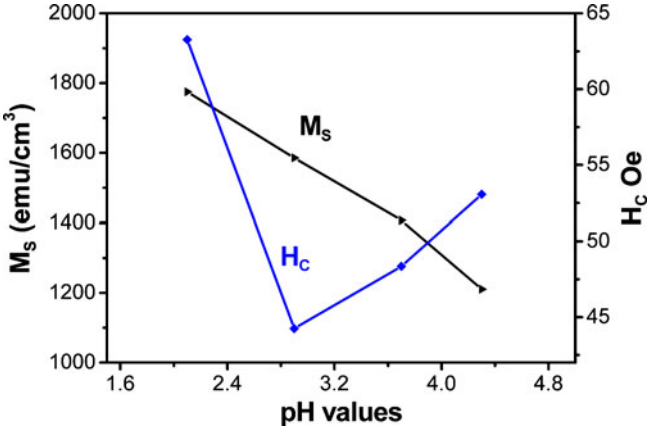

Figure 8. Dependence of saturation magnetization (M_s) and coercivity (H_c) of Fe–Ni films on pH value.

FeNi (200) and FeNi (211) of cubic structure. As shown in figure 6, the diffraction peaks of FeNi (110) shows stronger preferred orientation than that of FeNi (200) and FeNi (211) at any pH values. From the inset in figure 6, we can see that the diffraction peaks in the XRD patterns shift slightly towards high angles with increasing pH values, indicating decreasing lattice constant with increasing pH values. This can be attributed to the small atom radius of Fe (0·110 nm) as compared to the atom radium of Ni (0·162 nm). The incorporation of small atoms into the lattice of the film would shrink the lattice and decrease the lattice parameters (Kakatkar *et al* 1996; Tilak *et al* 1997).

3.2c *SEM analysis*: Figure 7 shows the surface morphology of the films deposited at different pH values from the electrolyte containing 0·12 M $NiSO_4{\cdot}6H_2O$ + 0·08 M $FeSO_4{\cdot}7H_2O$ + 0·4 M H_3BO_3 + 1·7 mM $C_6H_8O_6$ + 1·38 mM CH_4N_2S at room temperature. The surface morphology is strongly influenced by the electrolyte pH. The films prepared at low pH values (2·10 and 2·90) show a relatively smooth surface and smaller grains compared to those prepared at high pH values (3·70 and 4·50). It is clearly indicated that with the pH values increasing, the surface of the films become more rough. This change may be explained by the hydrogen evolution, which is favoured at low pH values. Recent studies also showed that deposition parameters, for example pH, affect the microstructure of electrodeposited metal films (Alper *et al* 2008; Kockar *et al* 2010; Qiang *et al* 2010; Tian *et al* 2011).

3.2d *Magnetic property analysis*: Dependence of M_S and H_C of the Fe–Ni films on the different pH values is shown in figure 8. It can be seen that the saturation magnetization (M_s) decreases from 1775·01 emu/cm^3 to 1501·46 emu/cm^3 with pH value increasing from 2·1 to 4·3. The coercivity (H_c) of the films slightly reduces from 63·27 Oe of pH 2·1 to 43·14 Oe of pH 2·9, and then increases with further increase in pH values. Coercivity (H_c) reaches a minimum value of 43·14 Oe at pH = 2·9. On the basis of the above results, decrease of saturation magnetization (M_s) is caused by the increase of Fe which has lower saturation magnetization (M_s) than Ni in the films. The coercivity (H_c) is sensitive to the phase, defect, stress and thickness of the films (Li *et al* 2008).

4. Conclusions

Fe–Ni films with different Ni content and morphology were successfully electrodeposited on ITO glass from the electrolytes containing both different Ni^{2+} and Fe^{2+} concentrations and different pH values without stirring. The content of nickel gradually increases from 38% to 84% as the mole ratio of $NiSO_4/FeSO_4$ varying from 0·50/0·50 to 0·90/0·10 in electrolyte and the content of Ni slightly decreases from 65% to 42% as the pH values vary from 2·1 to 4·3. The $Fe_{1-x}Ni_x$ films have the same structure with Ni content x increasing from 0·38 to 0·84. The XRD and morphology investigation indicate that films have similar structure. However, the films grown in high pH values (3·7 and 4·5) have larger grains compared to those prepared at low pH values (2·1 and 2·9). The magnetic performance of the films shows that the saturation magnetization (M_s) moves up from 1150·44 emu/cm^3 to 2498·88 emu/cm^3 with the increase of Ni^{2+} concentration in the electrolyte. The coercivity (H_c) decreases with the Ni content x increasing from 0·38 to 0·55, reaches a minimum value of 43·14 Oe at x = 0·55, and then increases with further increase of Ni^{2+} concentration in the electrolyte. The saturation magnetization (M_s) decreases from 1775·01 emu/cm^3 to 1501·46 emu/cm^3 with the pH value increasing from 2·1 to 4·3.

References

Alper M, Kockar H, Safak M and Baykul M C 2008 *J. Alloys. Compd.* **453** 15

Beltowska-Lenman E and Riesenkampf A 1980 *Surf. Technol.* **11** 349

Beltowska-Lehman E, Ozga P, Swiatek Z and Lupi C 2002 *Surf. Coat. Technol.* **444** 151

Chen Y and Sun I W 2001 *Electrochim. Acta* **46** 1169

Chisholm C, Kuzmann E, EI-Sharif M, Doyle O, Stichleutner S, Solymos K, Homonnay Z and Vertes A 2007 *Appl. Surf. Sci.* **253** 4348

Chueng C, Djuanda F, Erb U and Palumbo G 1994 *Mater. Sci. Eng.* **A85** 39

Chueng C, Palumbo G and Erb U 1994 *Scr. Metal. Mater.* **31** 735

Friemel F 1966 East German Patent 52869

Friemel F 1967 *Chem. Abstr.* **67** 17376

Gyftou P, Pavlatou E A and Spyrellis N 2008 *Appl. Surf. Sci.* **254** 5910

Harris T M, Wilson J L and Bleakley M 1999 *J. Electrochem. Soc.* **146** 1461

Jartych E, Jalochowiski M and Budzynski M 2002 *Appl. Surf. Sci.* **193** 210

Kakatkar S V, Kakatkar S S, Patil R S, Sankpal A M, Suryawanshi S S, Bhosale D N and Sawant S R 1996 *Phys. Status Solidi* **B198** 853

Kockar Hakan, Alper Mursel, Sahin Turgut and Karaagac Oznur 2010 *J. Magn. Magn. Mater.* **322** 1095

Korenivski V 2000 *J. Magn. Magn. Mater.* **215–216** 800

Krause T, Arulnayagam L and Pritzke M 1997 *J. Electrochem. Soc.* **144** 960

Li B S, Lin A, Wu X, Zhang Y M and Gan F X 2008 *J. Alloys. Compd.* **453** 93

Lieder M and Biallozor S 1985 *Surf. Technol.* **26** 23

Lodhi Z F, Mol J M C, Hamer W J, Terryn H A and DeWit J H W 2007 *Electrochim. Acta* **52** 5444

Marikkannu K R, Paruthimal Kalaignan G and Vasudevan T 2007 *J. Alloys Compd.* **438** 332

Matlosz M 1993 *J. Electrochem. Soc.* **140** 2271

Osaka T 1999 *Electrochem. Acta* **44** 3855

Osaka T, Takai M, Ohashi K, Saito M and Yamada K 1998 *Nature* **392** 796

Passal F 1966 US Patent 3274079

Passal F 1967 *Chem. Abstr.* **66** 16032

Qiang C W, Xu J C, Xiao S T, Jiao Y J, Zhang Z Q, Liu Y, Tian L L and Zhou Z G 2010 *Appl. Surf. Sci.* **257** 1371

Romankiw L T, Croll I M and Hatzakis M 1970 *IEEE Trans. Magn.* **6** 597

Sasaki K Y and Talbot J B 2000 *J. Electrochem. Soc.* **147** 189

Schwarzacher W and Lashmore D S 1996 *IEEE Trans. Hagn.* **MAG-32** 3133

Siritaratiwat A, Hill E W, Stutt I, Fallon J M and Grundy P J 2000 *Sensor Actuat. A: Phys.* **81** 40

Tian L L, Xu J C and Qiang C W 2011 *Appl. Surf. Sci.* **257** 4689

Tilak B V, Gendron A S and Mosoiu M A 1997 *J. Electrochem. Soc.* **7** 495

Valeri S, Giovanardi C, Borghi A, di Bona A and Luches P 2001 *Appl. Surf. Sci.* **175–176** 123

Venkatasetty H V 1970 *J. Electrochem. Soc.* **117** 403

Yin K M 1997 *J. Electrochem. Soc.* **144** 1560

Yin K M and Lin B T 1996 *Surf. Technol.* **78** 205

Zech Z, Podlaha E J and Landolt D 1999 *J. Electrochem. Soc.* **146** 2886

Zhang Y H and Ivey D L G 2004 *Chem. Mater.* **16** 1189